Pramana – J. Phys. (2020) 94:53
https://doi.org/10.1007/s12043-020-1917-x

Shell model description of the core excited level structure of ^{89}Sr nucleus and systematic features of the $N = 51$ odd-A isotones

YI HENG WU[1],*, KE YAN MA[2], FEI CHENG[1] and XUE YUAN CAI[1]

[1]School of Physics and Electronic Engineering, An Qing Normal University, Anqing, China
[2]College of Physics, Jilin University, Changchun, China
*Corresponding author. E-mail: wuyiheng2153306@163.com

MS received 13 March 2019; revised 1 July 2019; accepted 11 December 2019

Abstract. Shell-model calculations are performed using NuShellX code in the model space $\pi(f_{5/2}, p_{3/2}, p_{1/2}, g_{9/2}) \otimes \nu(g_{9/2}, g_{7/2}, d_{5/2}, h_{11/2})$, which probe the proton core excitation from the interior of $Z = 38$ semiclosed shell and neutron core excitation from the interior of $N = 56$ semiclosed shell for the level structure of ^{89}Sr. Our calculations show that the excitation of a single $d_{5/2}$ neutron across $N = 56$ semiclosed shell into the $h_{11/2}$ orbit should have great effects on the excited states of ^{89}Sr. In addition, the systematic features of proton core excitation across $Z = 38$ semiclosed shell into the $g_{9/2}$ orbit and neutron core excitation across $N = 56$ semiclosed shell into the $g_{7/2}, s_{1/2}, d_{3/2}, h_{11/2}$ orbits in $N = 51$ isotones are discussed.

Keywords. Level structure; shell model; core excitation.

PACS Nos **21.10.Pc; 25.70.Jj; 21.60.Cs; 27.60.+j**

1. Introduction

Nuclei around the closed proton and neutron shells play a key role in nuclear physics [1–9]. A large number of studies showed that nuclei in $A \sim 90$ ($Z \sim 38$, $N \sim 50$) mass region provide suitable objects to probe into the effects of nucleon excitations in the level structures, especially for the proton and neutron core excitation. Until recently, the breaking of the neutron core and proton core in Sr, Y, Zr, Nb, Mo, Tc, Ru and Rh nuclei have been interpreted by the shell model in $A \sim 90$ ($Z \sim 38$, $N \sim 50$) region [1,2,10–15]. In those nuclei, the low-lying levels are proposed to be understood as the transition of protons from the $f_{5/2}$ and $p_{3/2}$ orbits into the $p_{1/2}$ and $g_{9/2}$ orbits, and the high spin states are characterised by one $g_{9/2}$ neutron transition from the interior of $N = 50$ closed shell into the $d_{5/2}$ orbital. For example, shell-model investigations of nuclei with $N = 51$ are usually carried out with $\pi(f_{5/2}, p_{3/2}, p_{1/2}, g_{9/2}) \otimes \nu(g_{9/2}, g_{7/2}, d_{5/2}, d_{3/2}, s_{1/2})$ model space. A restricted model space adopted from the fpg orbitals for protons and gds orbitals for neutrons is considered [16–18]. Most of the experimentally established levels of those nuclei can be explained in this model space. However, some calculated levels are not in good agreement with experimental ones. In fact, the high spin levels were considered as $d_{5/2}$ neutron core excitation (a single $d_{5/2}$ neutron transition from the interior of $N = 56$ semimagic shell closure into the $h_{11/2}$ orbit) in $N = 51$ isotones ^{91}Zr [19], ^{93}Mo [20], ^{94}Tc [21], ^{95}Ru [22]. The $27/2_2^-$ state at 6770 keV in ^{91}Zr was described by the competition between proton across $Z = 38$ semimagic shell closure and neutron across $N = 56$ semimagic shell closure. In addition, the generation mechanisms of high spin levels without neutron transition from the interior of $N = 50$ closed shell into $g_{9/2}$ orbit but neutron transition from the interior of $N = 56$ semimagic shell closure is investigated in ^{95}Ru. In these nuclei, the model space $\pi(f_{5/2}, p_{3/2}, p_{1/2}, g_{9/2}) \otimes \nu(g_{9/2}, g_{7/2}, d_{5/2}, d_{3/2}, s_{1/2}, h_{11/2})$ was adopted to describe the experimentally established levels. The results agree well with the experimental ones, which indicated that the $d_{5/2} \rightarrow h_{11/2}$ neutron core excitation is necessary and important.

Prior study on ^{89}Sr was based on shell-model calculations with only proton core excitation taken into consideration, but the breakup of $N = 56$ core was not investigated [18]. According to the analogy of the level schemes with its isotones ^{91}Zr, ^{93}Mo, ^{94}Tc, ^{95}Ru, the $d_{5/2} \rightarrow h_{11/2}$ neutron core excitation should be considered to further explore the mechanisms of nucleon core excitation in ^{89}Sr. The goal of our study is to verify the capabilities of reproducing the experimental data of

Published online: 12 March 2020

Table 1. The single particle energies (SPEs) corresponding to the model space SNE.

L_j	$f_{5/2}$	$p_{3/2}$	$p_{1/2}$	$g_{9/2}$	$g_{7/2}$	$d_{5/2}$	$d_{3/2}$	$s_{1/2}$	$h_{11/2}$
ϵ_π (MeV)	0.5250	1.2280	5.1060	5.5180	20.6560	18.8930	20.0160	16.8950	
ϵ_ν (MeV)	0.0000	0.0000	0.0000	0.0000	4.3520	2.3130	3.4400	1.5320	−0.5890

the excited states of ^{89}Sr for the model spaces with and without $\nu h_{11/2}$.

2. Shell-model calculations

The experimentally established levels of ^{89}Sr are investigated by the shell model with two configuration spaces (SM-I and SM-II). The calculations adopt the NuShellX code with the SNE model space and the SNET residual interaction [23]. The model space consists of eight proton orbits $\pi(f_{5/2}, p_{3/2}, p_{1/2}, g_{9/2}, g_{7/2}, d_{5/2}, d_{3/2}, s_{1/2})$ and nine neutron orbits $\nu(f_{5/2}, p_{3/2}, p_{1/2}, g_{9/2}, g_{7/2}, d_{5/2}, d_{3/2}, s_{1/2}, h_{11/2})$. The single-particle energies (SPEs) corresponding to the model space are shown in table 1.

For the two configuration spaces, truncations are performed in the calculations on the basis of similar level schemes introduced in refs [12,17,18,21,22]. In our truncations, the protons are redistributed in the $\pi(f_{5/2}, p_{3/2}, p_{1/2}, g_{9/2})$ orbits, and the neutrons are completely filled in $\nu(f_{5/2}, p_{3/2}, p_{1/2})$ orbits. Besides that, for the SM-I configuration space, $g_{9/2}$ neutron transition from the interior of $N = 50$ shell closure into $g_{7/2}$ orbit is considered. For the SM-II configuration space, not only $g_{9/2}$ neutron transition from the interior of $N = 50$ shell closure to $g_{7/2}$ orbit but also neutron transition from the interior of $N = 56$ subshell closure to the $h_{11/2}$ orbit are considered.

3. Results and discussion

The present results are compared with those of the experiments in ref. [18], as shown in figure 1. The calculation results are shown in tables 2 and 3. One can see from figure 1, that the results with the SM-II configuration space (considered $d_{5/2} \rightarrow h_{11/2}$ neutron core excitation) give better agreement with the experiments than with SM-I ($d_{5/2} \rightarrow h_{11/2}$ neutron core excitation is not considered). This indicates that the contributions of neutron core excitation ($d_{5/2} \rightarrow h_{11/2}$) should be considered to interpret the spin states of ^{89}Sr. The results will be discussed in detail with the configuration space SM-II. As shown in table 3, the ground-state $5/2^+$ is dominated

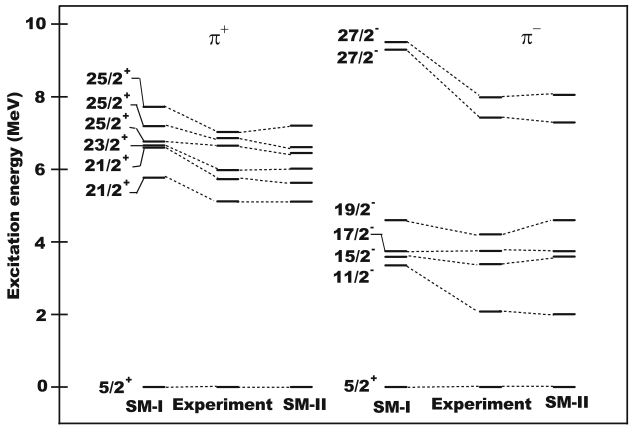

Figure 1. Comparison between experimental levels in ref. [18] and the calculated energy levels in ^{89}Sr within SM-I and SM-II configuration spaces.

by the $\nu d_{5/2}$ configuration. It is evident from table 3 that the neutron core excitation ($d_{5/2} \rightarrow h_{11/2}$) appears in the positive parity states from $21/2^+_1$ to $25/2^+_1$. The main wave function of the $21/2^+_1$ and $23/2^+$ states is $\pi(p^{-1}_{3/2} g_{9/2} \otimes \nu h_{11/2})$. The main wave function of the $21/2^+_2$ and $25/2^+_1$ states is $\pi(f^{-1}_{5/2} g_{9/2} \otimes \nu h_{11/2})$. However, with the increase of the excitation energy and angular momentum, the neutron core excitation ($d_{5/2} \rightarrow h_{11/2}$) disappears at the $25/2^+_2$ and $25/2^+_3$ states with excitation energies of ∼7 MeV. Besides, an additional $f_{5/2}$ or $p_{3/2}$ proton transition from the interior of $Z = 38$ subshell closure into the $g_{9/2}$ orbital appears at the $25/2^+_2$ and $25/2^+_3$ states. The $25/2^+_2$ state is mainly made by a proton pair transition from the $f_{5/2}$ orbit across $Z = 38$ subshell closure into the $g_{9/2}$ orbital with the configuration $\pi(f^{-2}_{5/2} g^2_{9/2} \otimes \nu d_{5/2})$. The $25/2^+_3$ state arises from the transition of $f_{5/2}$ and $p_{3/2}$ protons from the interior of $Z = 38$ subshell closure with the configuration $\pi(f^{-1}_{5/2} p^{-1}_{3/2} g^2_{9/2} \otimes \nu d_{5/2})$.

The $11/2^-$ state at 2079 keV is nicely reproduced with only a deviation of 68 keV from SM-II configuration space. The $11/2^-$ state is dominated by the configuration in which the single $\nu d_{5/2}$ neutron is promoted from the interior of $N = 56$ subshell closure into the $\nu h_{11/2}$ orbit. In SM-I configuration space, the $11/2^-$ state is dominated by a single $d_{5/2}$ neutron

Table 2. Leading components of the wave functions for the states of ^{89}Sr with SM-I configuration space. The wave functions for a particular state may include several components, where each component is of the form $p = [\pi(p(1), p(2), p(3), p(4)) \otimes \nu(n(1), n(2), n(3), n(4))]$. Here $p(i)$ represents the proton number in the $(f_{5/2}, p_{3/2}, p_{1/2}, g_{9/2})$ orbits and $n(j)$ represents neutron number in the $(p_{1/2}, g_{9/2}, g_{7/2}, d_{5/2})$ orbits.

I^{π} ($\hbar$)	E_{exp} (keV)	E_{cal} (keV)	Wave function ($\pi \otimes \nu$)	Components (%)
$5/2^+$	0	0	6 4 0 0 $\otimes$ 2 10 0 1	50.7
			6 2 2 0 $\otimes$ 2 10 0 1	11.4
$21/2_1^+$	5115	5768	4 4 0 2 $\otimes$ 2 10 0 1	41.34
			5 3 0 2 $\otimes$ 2 10 0 1	18.45
			6 2 0 2 $\otimes$ 2 10 0 1	16.09
$21/2_2^+$	5726	6661	5 3 0 2 $\otimes$ 2 10 0 1	43.17
			4 4 0 2 $\otimes$ 2 10 0 1	27.62
			6 2 0 2 $\otimes$ 2 10 0 1	16.09
$23/2^+$	5797	6763	5 3 0 2 $\otimes$ 2 10 0 1	14.64
			4 3 1 2 $\otimes$ 2 10 0 1	7.61
			6 2 0 2 $\otimes$ 2 10 0 1	16.09
$25/2_1^+$	6650	6595	4 4 0 2 $\otimes$ 2 10 0 1	69.99
			4 3 1 2 $\otimes$ 2 10 0 1	9.75
$25/2_2^+$	6857	7192	5 3 0 2 $\otimes$ 2 10 0 1	60.65
			5 2 1 2 $\otimes$ 2 10 0 1	14.95
$25/2_3^+$	7026	7722	5 3 0 2 $\otimes$ 2 10 0 1	49.86
			5 2 1 2 $\otimes$ 2 10 0 1	13.25
			6 2 0 2 $\otimes$ 2 10 0 1	8.88
$11/2^-$	2079	3357	6 3 0 1 $\otimes$ 2 10 0 1	61.46
			5 4 0 1 $\otimes$ 2 10 0 1	19.28
$15/2^-$	3389	3590	6 3 0 1 $\otimes$ 2 10 0 1	56.82
			5 3 1 1 $\otimes$ 2 10 0 1	6.41
			6 2 1 1 $\otimes$ 2 10 0 1	6.01
$17/2^-$	3751	3742	5 4 0 1 $\otimes$ 2 10 0 1	69.98
			5 2 0 3 $\otimes$ 2 10 0 1	5.09
			5 2 2 1 $\otimes$ 2 10 0 1	4.45
$19/2^-$	4209	4597	5 4 0 1 $\otimes$ 2 10 0 1	64.27
			4 4 1 1 $\otimes$ 2 10 0 1	6.75
			5 2 0 3 $\otimes$ 2 10 0 1	5.66
$27/2_1^-$	7422	9269	5 4 0 1 $\otimes$ 2 9 0 2	67.80
$27/2_2^-$	7984	9503	5 4 0 1 $\otimes$ 2 9 1 1	37.34
			5 4 0 1 $\otimes$ 2 9 0 2	25.07

coupled to the $p_{3/2}$ proton excitation from the interior of $Z = 38$ subshell closure into the $g_{9/2}$ orbit, leading to the configuration $\pi(p_{3/2}^{-1} g_{9/2}) \otimes \nu d_{5/2}$, whereas the calculated level energy of the $11/2^-$ state is almost 1.3 MeV higher than the experimental value. As described above, the excitation of neutron core ($d_{5/2} \rightarrow h_{11/2}$) seems to be more reasonable to describe the $11/2^-$ state of ^{89}Sr, comparing the excitation of proton core ($p_{3/2} \rightarrow g_{9/2}$). For the $15/2^-$, $17/2^-$ and $19/2^-$ states, the shell-model calculations with SM-I and II are both consistent with the experimental data. The main configuration of $15/2^-$ is $\pi(p_{3/2}^{-1} g_{9/2}) \otimes \nu d_{5/2}$. For the $17/2^-$ and $19/2^-$ states, the main configuration is $\pi(f_{5/2}^{-1} g_{9/2}) \otimes \nu d_{5/2}$. It should be noted that the spin and parity of experimental 7984 keV level was not assigned in ref. [18]. That this experimental energy level only decays into the $25/2$ energy level and coincides with the calculated level $27/2^-$ in SM-II configuration space has to be taken into consideration. The state has a dominant contribution from the $\pi(f_{5/2}^{-1} p_{3/2}^{-1} g_{9/2}^2) \otimes \nu h_{11/2}$ configuration. Here, we temporarily proposed this state as $27/2^-$. As discussed above, the results may indicate that the single $d_{5/2}$ neutron across $N = 56$ subshell closure into the $\nu h_{11/2}$ orbit is essential to reproduce the experimental ones in ^{89}Sr nucleus. The present level structure of ^{89}Sr nucleus is generated by three mechanisms: (a) the single proton transition from the $f_{5/2}$ or $p_{3/2}$ orbital crosses $Z = 38$ subshell closure to the $g_{9/2}$ orbital; (b) two-proton transitions from the $f_{5/2}$ and $p_{3/2}$ orbits cross $Z = 38$ subshell closure to the $g_{9/2}$ orbit; (c) the single neutron transition from the

Table 3. Similar to table 2 but with SM-II configuration space. Here $n(j)$ represents the neutron number in the $g_{9/2}$, $g_{7/2}$, $d_{5/2}$, $h_{11/2}$ orbits.

I^π ($\hbar$)	E_{exp} (keV)	E_{cal} (keV)	Wave function ($\pi \otimes \nu$)	Components (%)
$5/2^+$	0	0	6 4 0 0 ⊗ 10 0 1 0	56.86
			6 2 2 0 ⊗ 10 0 1 0	11.34
$21/2_1^+$	5115	5110	6 3 0 1 ⊗ 10 0 0 1	56.92
			4 3 2 1 ⊗ 10 0 0 1	8.44
			5 3 1 1 ⊗ 10 0 0 1	7.92
$21/2_2^+$	5726	5626	5 4 0 1 ⊗ 10 0 0 1	53.13
			6 2 0 0 ⊗ 10 1 0 0	11.58
$23/2^+$	5979	6017	6 3 0 1 ⊗ 10 0 0 1	60.11
			5 3 2 0 ⊗ 10 1 0 0	21.33
$25/2_1^+$	6650	6446	5 4 0 1 ⊗ 10 0 0 1	60.83
			4 4 1 1 ⊗ 10 0 0 1	6.66
			5 2 0 3 ⊗ 10 0 0 1	5.98
$25/2_2^+$	6857	6610	4 4 0 2 ⊗ 10 0 1 0	66.79
			4 3 1 2 ⊗ 10 0 1 0	8.99
			5 2 0 3 ⊗ 10 0 1 0	3.40
$25/2_3^+$	7026	7200	5 3 0 2 ⊗ 10 0 1 0	60.28
			5 2 1 2 ⊗ 10 0 1 0	14.98
$^*27/2^+$	–	7744	4 4 0 2 ⊗ 10 0 1 0	51.86
			5 3 0 2 ⊗ 10 0 1 0	19.09
			4 3 1 2 ⊗ 10 0 1 0	9.95
$^*29/2^+$	–	8199	4 4 0 2 ⊗ 10 0 1 0	53.17
			5 3 0 2 ⊗ 10 0 1 0	17.15
			4 3 1 2 ⊗ 10 0 1 0	13.04
$^*31/2^+$	–	9407	4 4 0 2 ⊗ 10 1 0 0	70.40
			4 3 1 2 ⊗ 10 1 0 0	14.55
$^*33/2^+$	–	10316	5 4 0 1 ⊗ 9 0 1 1	69.23
			4 3 1 2 ⊗ 10 1 0 0	14.55
$11/2^-$	2079	2011	6 4 0 0 ⊗ 10 0 0 1	54.79
			6 2 2 0 ⊗ 10 0 0 1	19.20
$15/2^-$	3389	3596	6 3 0 1 ⊗ 10 0 1 0	56.51
			4 3 2 1 ⊗ 10 0 1 0	10.38
$17/2^-$	3751	3745	5 4 0 1 ⊗ 10 0 1 0	69.76
			5 2 0 3 ⊗ 10 0 1 0	5.13
$19/2^-$	4209	4599	5 4 0 1 ⊗ 10 0 1 0	64.05
			4 4 1 1 ⊗ 10 0 1 0	6.71
$27/2_1^-$	7422	7293	4 4 0 2 ⊗ 10 0 0 1	34.86
			6 2 0 2 ⊗ 10 0 0 1	23.84
			5 3 0 2 ⊗ 10 0 0 1	15.43
$27/2_2^-$	7984	8052	5 3 0 2 ⊗ 10 0 0 1	52.46
			4 4 0 2 ⊗ 10 0 0 1	21.66
$^*29/2^-$	–	8226	5 3 0 2 ⊗ 10 0 0 1	56.51
			5 2 1 2 ⊗ 10 0 0 1	12.10
$^*33/2^-$	–	9361	5 4 0 1 ⊗ 10 0 0 1	45.98
			5 3 0 2 ⊗ 10 0 0 1	22.50
$^*37/2^-$	–	12201	4 4 0 2 ⊗ 10 0 0 1	62.78
			5 3 0 2 ⊗ 9 0 1 1	9.56

$d_{5/2}$ orbit crosses $N = 56$ subshell closure to the $h_{11/2}$ orbit. Even the combination of these mechanisms are involved.

It is noteworthy that the breakup of $N = 50$ core should be fully taken into account in generating high spin states in $A \sim 90$ ($Z \sim 38$, $N \sim 50$) mass region. For the nucleus ^{89}Sr, the similarity characteristic should be observed in its high spin states. However, the mechanism of the breakup of $N = 50$ core has not been observed in the present experimental levels ($J^\pi \leq 25/2_3^+$ and $J^\pi \leq 27/2_2^-$). It is worth mentioning that the configurations of several states ($J^\pi >$

$25/2_3^+$ and $J^\pi > 27/2_2^-$) with the shell-model calculations are marked by asterisks, as shown in table 3. The first $33/2^+$ level at 10316 keV and the first $37/2^-$ level at 12201 keV involve the breaking of $N = 50$ shell closure, namely, a single $\nu g_{9/2}$ neutron transition from the interior of $N = 50$ shell closure into the $\nu g_{7/2}$ orbit. So, it is anticipated that the mechanism of the breaking of $N = 50$ core will play a key role by increasing the excitation energy in ^{89}Sr. More measurements are necessary for exploring the excitation of neutrons from the interior of $N = 50$ and 56 shell gaps.

4. The systematic features of $N = 56$ neutron core excitation and $Z = 38$ proton core excitation in $N = 51$ isotones

To further understand the systematic features of the proton and neutron core excitations, the systematic features of $N = 56$ neutron core and $Z = 38$ proton core excitation in the $N = 51$ isotones from the ^{85}Se to ^{97}Pd nuclei are displayed in figures 2 and 3, where the data are taken from refs [24–30]. The energies of the first $7/2^+$, $3/2^+$, $1/2^+$ and $11/2^-$ states attribute to a $d_{5/2}$ neutron transition from the interior of $N = 56$ subshell closure into the $g_{7/2}$, $d_{3/2}$, $s_{1/2}$ and $h_{11/2}$ orbits, which are connected by dashed red lines. As can seen from figure 2, the excitation energies of $1/2^+$ and $7/2^+$ states increase at first and then decrease with the increasing proton numbers in the $\pi g_{9/2}$ orbit, a maximum shows up at $Z = 40$. This may be due to the fact that the wave function overlap between the spin-orbit-partner $\pi g_{9/2}$ and $\nu(g_{7/2}, s_{1/2})$ orbits may cause an interplay

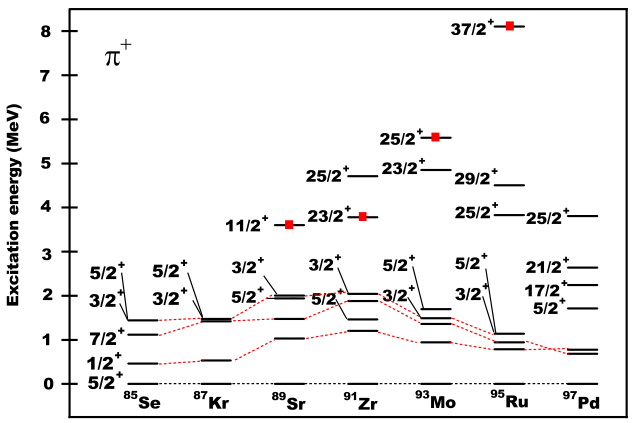

Figure 2. Excitation energies for the states from the $\nu d_{5/2}$ orbit to the $\nu(g_{7/2}, d_{3/2}, s_{1/2})$ orbits across $N = 56$ subshell closure were connected by red dash lines and proton core excitations from the $\pi f_{5/2}$ orbit to the $\pi g_{9/2}$ orbit across $Z = 38$ subshell closure were marked by red square dots.

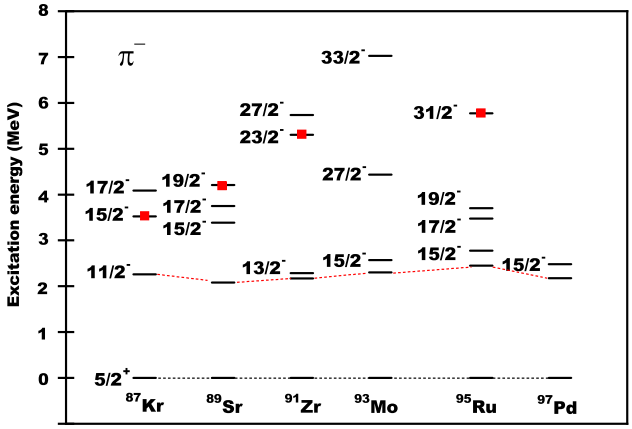

Figure 3. Excitation energies for the states from the $\nu d_{5/2}$ orbit to the $\nu h_{11/2}$ orbit across $N = 56$ subshell closure were connected by red dash line and proton core excitations from the $f_{5/2}$ orbit to the $g_{9/2}$ orbit across $Z = 38$ subshell closure were marked by red square dots.

between proton and neutron [31]. And the interplay between $\pi g_{9/2}$ and $\nu(g_{7/2}, s_{1/2})$ may exhibit characteristics similar to the behaviour of the excitation energies of $1/2^+$ and $7/2^+$ states. In addition, the energy gaps between the $d_{5/2}$ and $s_{1/2}$ neutron orbits increase at first and then decrease with increasing proton numbers in $\pi g_{9/2}$ orbit, and it is maximum at $Z = 40$. These phenomena seem to be significant for investigating the shell evolution and more detailed investigations should be carried out in the future. Figures 2 and 3 show the systematic features of the breaking of $Z = 38$ core from ^{89}Sr to ^{97}Pd nuclei. The energies of proton core excitation increase as the number of protons increase in the $\pi g_{9/2}$ orbit. It is noteworthy that the excitation energy of the $(d_{5/2} \rightarrow g_{7/2})$ for the ^{89}Sr nucleus is very close to the ^{87}Kr nucleus. The explanation could be that the ^{87}Kr nucleus has 36 protons, two less than that of the ^{89}Sr nucleus, their proton Fermi levels should be very close and far away from the $\pi g_{9/2}$ orbit, while the proton Fermi level of ^{91}Zr lies at the $\pi p_{1/2}$ orbital, close to the $\pi g_{9/2}$ orbital. As shown in figure 3, the $N = 56$ neutron core excitation, i.e., a single $d_{5/2}$ neutron transition from the interior of $N = 56$ subshell closure into the $h_{11/2}$ orbit, is included in the present systematic investigation. There is no strong evolution in the relative SPE between the $d_{5/2}$ and $h_{11/2}$ orbits. Similar characteristic is also observed in the $N = 51$ odd–odd isotones [7,17,30]. In these nuclei, the energies of the 10^- states are almost not changed at about 2 MeV. These may be due to the fact that the poor radial overlap between $\pi g_{9/2}$ proton orbit and $\nu h_{11/2}$ neutron orbit tempers the interactions between $\pi g_{9/2}$ proton orbit and $\nu h_{11/2}$ neutron orbit and leaves a somewhat similar change in the binding energy between them.

5. Conclusion

Shell-model calculations containing the $d_{5/2}$ neutron excitation from the interior of $N = 56$ subshell closure into the $g_{7/2}$, $h_{11/2}$ orbits are executed to explain the energy spectra structure based on the experiment of ^{89}Sr nucleus. It is confirmed that the excitation of neutron across $N = 56$ subshell closure is essential for the description of the level structure of ^{89}Sr nucleus. In addition, the $N = 50$ core excitation is another plausible mechanism for generating higher angular momentum states. Moreover, the evolution characteristics of the $N = 56$ neutron and $Z = 38$ proton core excitation in the $N = 51$ isotones are investigated. It is anticipated that these evolution characteristics will be observed in future experiments and may play a key role in the spectra with $N = 51$ isotones in the $A \sim 90$ ($Z \sim 38$, $N \sim 50$) mass region.

Acknowledgements

This work was supported by the National Natural Science Foundation of China under Grant Nos 11775098 and 11405072, Jilin Scientific and Technological Development Program Nos 20190201137JC and 20180520195JH, the 13th Five-Year Plan of Scientific Research of Jilin Province No. JJKH20180117 and China Postdoctoral Science Foundation Nos 2015M571354 and 2013M541285, the Key Program of the Education Department of Anhui Province under Grant Nos KJ2017A369 and KJ2017A365. Computations were carried out on the server hosted by the School of Physics and Electronic Engineering of An Qing Normal University.

References

[1] D P Ahalpara and K H Bhatt, *Pramana – J. Phys.* **6**, 222 (1976)
[2] R Sahu and V K B Kota, *Pramana – J. Phys.* **82**, 757 (2014)
[3] Monica Karday *et al*, *Pramana – J. Phys.* **91**: 70 (2018)
[4] Han-Kui Wang *et al*, *Phys. Rev. C* **96**, 054313 (2017)
[5] Yue Shi, *Phys. Rev. C* **95**, 034307 (2017)
[6] L Olivier *et al*, *Phys. Rev. L* **119**, 192501 (2017)
[7] Y H Wu *et al*, *Chin. Phys. Lett.* **31**, 042101 (2014)
[8] F Flavigny *et al*, *Phys. Rev. L* **118**, 242502 (2017)
[9] D Steppenbeck *et al*, *Phys. Rev. C* **96**, 064310 (2017)
[10] Z Q Li *et al*, *Phys. Rev. C* **94(3)**, 014315 (2016)
[11] E A Stefanova *et al*, *Phys. Rev. C* **62**, 054314 (2001)
[12] A Chakraborty *et al*, *Phys. Rev. C* **72**, 054309 (2005)
[13] P W Luo *et al*, *Phys. Rev. C* **89**, 034318 (2014)
[14] S E Arnell *et al*, *Phys. Rev. C* **49(1)**, 51 (1994)
[15] Rui Ju Guo *et al*, *Chin. Phys. C* **41**, 084105 (2017)
[16] G Rainovski *et al*, *Phys. Rev. C* **65**, 044327 (2002)
[17] S S Ghugre *et al*, *Phys. Rev. C* **51**, 2809 (1995)
[18] E A Stefanova *et al*, *Phys. Rev. C* **63**, 064315 (2001)
[19] L He *et al*, *Sci. Sin-Phys. Mech. Astron.* **42(3)**, 249 (2012)
[20] T Fukuchi *et al*, *Eur. Phys. J. A* **24**, 249 (2005)
[21] S S Ghugre *et al*, *Phys. Rev. C* **61**, 024302 (1999)
[22] E Galindo *et al*, *Phys. Rev. C* **69**, 024304 (2004)
[23] B A Brown and W D M Rae, Nushell@MSU, MSU-NSCL report (2007)
[24] Balraj Singh, *Nuclear Data Sheets* **114**, 1 (2013)
[25] Coral M Baglin, *Nuclear Data Sheets* **112**, 1163 (2011)
[26] Coral M Baglin, *Nuclear Data Sheets* **116**, 1 (2014)
[27] Coral M Baglin, *Nuclear Data Sheets* **114**, 1293 (2013)
[28] Coral M Baglin, *Nuclear Data Sheets* **111**, 525 (2010)
[29] M G Porquet *et al*, *Eur. Phys. J. A* **28**, 153 (2006)
[30] W F Piel *et al*, *Phys. Rev. C* **41**, 1223 (1990)
[31] P Federman and S Pittel, *Phys. Lett. B* **69**, 385 (1977)